International Journal of Chemical, Materials and Biomolecular Sciences
ISSN: 2415-6620
Vol:6, No:1, 2012

# Structure and Magnetic Properties of Nanocomposite $Fe_2O_3/TiO_2$ Catalysts Fabricated by Heterogeneous Precipitation

Jana P. Vejpravova, Daniel Niznansky, Vaclav Vales, Barbara Bittova, Vaclav Tyrpekl, Stanislav Danis, Vaclav Holy, Stephen Doyle

***Abstract*—** The aim of our work is to study phase composition, particle size and magnetic response of $Fe_2O_3/TiO_2$ nanocomposites with respect to the final annealing temperature. Those nanomaterials are considered as smart catalysts, separable from a liquid/gaseous phase by applied magnetic field. The starting product was obtained by an ecologically acceptable route, based on heterogeneous precipitation of the $TiO_2$ on modified $\gamma$-$Fe_2O_3$ nanocrystals dispersed in water. The precursor was subsequently annealed on air at temperatures ranging from 200 $^oC$ to 900 $^oC$. The samples were investigated by synchrotron X-ray powder diffraction (S-PXRD), magnetic measurements and Mössbauer spectroscopy. As evidenced by S-PXRD and Mössbauer spectroscopy, increasing the annealing temperature causes evolution of the phase composition from anatase/maghemite to rutile/hematite, finally above 700 $^oC$ the pseudobrookite ($Fe_2TiO_5$) also forms. The apparent particle size of the various $Fe_2O_3/TiO_2$ phases has been determined from the high-quality S-PXRD data by using two different approaches: the Rietveld refinement and the Debye method. Magnetic response of the samples is discussed in considering the phase composition and the particle size.

***Keywords*—**X-ray diffraction, profile analysis, Mössbauer spectroscopy, magnetic properties, $TiO_2$, $Fe_2O_3$, $Fe_2TiO_5$

## I. Introduction

THE $TiO_2$-based nanomaterials are well known candidates for photocatalytic decomposition of toxic organic pollutants in water and air by means of heterogeneous *photocatalysis* [1-4]. In contrast to the pure $TiO_2$ phases, with active absorption in the UV region, the iron-doped $TiO_2$ or mixed Ti/Fe oxides are reported to be photoactive in the presence of visible light [1]. It has been also demonstrated that addition of $TiO_2$ to $Fe_2O_3$ leads to favorable impact of its electrochemical properties in Li ion batteries [5]. Therefore, the $TiO_2$-$Fe_2O_3$ based systems are of great interest due to the variety of application and ecological compatibility.

In order to keep the most effective photocatalytic performance of the catalyst, several material parameters, mainly the phase composition and particle size, must be carefully considered. In our work, we focused on investigation of those parameters in the $TiO_2$/ $Fe_2O_3$ nanocomposite system, obtained by a 'green' fabrication route [6]. The nanocomposite was designed as a smart catalyst, which can be separated from a liquid/gaseous phase by application of external magnetic field, and consist of a magnetically active core ($Fe_2O_3$) and the photoactive coating ($TiO_2$). We have prepared a series of nanocomposite samples, differing in the temperature of the final heat treatment, and investigated them by synchrotron powder X-ray diffraction, Mössbauer spectroscopy and magnetic measurements. The main goal was to demonstrate evolution of the phase composition and particle size of particular oxide phases with respect to the annealing temperature. The results are discussed in context of the considered application as magnetically separable photocatalysts.

J.P. Vejpravova and B. Bittova are with the Institute of Physics AS CR, v.v.i., Na Slovance 2, 18221 Prague 8, Czech Republic (e-mail: vejpravo@fzu.cz).

D. Niznansky and V. Tyrpekl are with the Charles University Prague, Faculty of Science, Hlavova 2, 12814 Prague 2, Czech Republic.

V. Vales, S. Danis and V. Holy are with the Charles University Prague, Faculty of Mathematics and Physics, Ke Karlovu 5, 12116 Prague 2, Czech Republic.

S. Doyle is with the Institut für Synchrotronstrahlung, Hermann-von-Helmholtz-Platz 1, D-76344 Eggenstein, Leopoldshafen, Germany.

## II. Experimental

### A. Sample preparation

The starting nanocomposite has been obtained by using an environment friendly approach, excluding toxic and expensive organic reactants described in detail in our previous work [6]. The preparation route is based on precipitation of the positively charged $TiO_2$ layer on negatively charged $\gamma$-$Fe_2O_3$ nanocrystals, modified by citric acid using a homogeneous hydrolysis of a metallic salt solution by urea. The obtained product, dried at 200 $^oC$ on air was subsequently annealed on air for one hour at the following temperatures: 400 $^oC$, 550 $^oC$, 700 $^oC$, 770 $^oC$, 820 $^oC$ and 900 $^oC$. The samples were labeled according to the final heat treatment temperature as S200 – S900.

### B. Powder X-ray diffraction and data analysis

The powder X-ray diffraction experiments were performed at the PDIFF beamline (ANKA synchrotron) in the Bragg – Brentano geometry using the wavelength of 1.00789 Å. The primary beam was monochromatized and the diffracted radiation was measured by a point detector equipped with analyzer. The experimental data were analyzed by two different approaches. First, the *Debye* formula (1) for the diffracted intensity, $I(Q)$ has been used for modeling the diffraction patterns [7]. In order to speed up the calculation procedure, the Debye formula was applied in the form including the distribution function of atomic pair distances [8]:

$$I(Q) = \sum_{a,b} f^a f^{b*} \sum_i m_i^{a,b} \frac{\sin(Qr_i^{ab})}{Qr_i^{ab}}, \quad (1)$$

where $Q$ is the length of the scattering vector, $f^a$ $f^b$ are the scattering factors of atoms $a$, $b$ (Ti-Ti, O-O and Fe-O etc.), $r_i$ is the $i$-th inter-atomic distance of the atom pair $a$, $b$, which appears $m_i$ times in the distance distribution function. The resulting parameters obtained from the model are the particle diameter (size), $d$ of each phase considered, and relative ratio of the phases. We analyzed only those samples with binary

oxide phases. Second, a generalized *Rietveld* refinement, implemented in the *FullProf/WinPlotr* software [9] was applied. The observed experimental pattern is considered as a convolution of the instrumental and intrinsic (sample) profile, and the fit (not limited to the number of phases) yields the particle diameter(s), *d*. The instrumental function of the diffractometer has been determined from the data recorded on the $LaB_6$ standard. The particle diameter of the well crystalline samples (S820 and S900) was not analyzed, as both procedures are limited to particles with size below approx. 80 nm.

### *C. Mössbauer spectroscopy*

The Mössbauer spectra were recorded in the transmission mode with $^{57}$Co diffused into a Rh matrix as the source moving with constant acceleration. The spectrometer was calibrated on a standard α–Fe foil and the isomer shift was expressed with respect to the standard at 293 K. The spectra of the S900 sample were also measured at 4.2 K, and under applied magnetic field of 6 T. The fitting of the spectra was performed using the NORMOS program.

### *D. Magnetic characterization*

Magnetic measurements were performed using MPMS 7XL (SQUID) device (Quantum Design, San Diego) in the temperature range 2 – 400 K. The temperature dependence of magnetization was recorded in the zero-field-cooled (ZFC) and field-cooled (FC) regime in the external magnetic field of 0.01 T. The temperature dependence of the a.c. susceptibility has been measured using the a.c. field amplitude of 3 *m*T and frequencies varying from 1 Hz to 1 *k*Hz.

## III. Results and Discussion

### *A. Powder X-ray diffraction and data analysis*

Results of the Debye analysis of the S-PXRD data are summarized in Table I. The relative content of the phases has been analyzed considering the $Fe_2O_3$ and $TiO_2$ binaries only. The starting material, S200 consists of the maghemite and almost identical amount of the anatase and rutile. While the content of maghemite is reduced with annealing, formation of the hematite phase propagates. The content of the $TiO_2$ phases has no clear trend. The samples annealed above 770 $^{o}$C consist of the hematite and the pseudobrookite phase only.

The evolution of particle size obtained from the Rietveld analysis is presented in Table II. The particle size of the $TiO_2$ phases does not change significantly, the maghemite particle size increases only by 2 nm, however, the hematite nanocrystallites grow from 7 to 24 nm when changing the temperature from 550 $^{o}$C to 770 $^{o}$C. The high-temperature samples (S820, S900) are well crystalline; therefore the particle size was not determined, as explained in the Section II. As an example, the measured data together with the Rietveld fit and Bragg positions of the corresponding phases are presented in Figure 1.

The observed behavior suggests, that up to 550 $^{o}$C, the morphology of the nanocomposite is mostly conserved, however when increasing the heating temperature the interaction of the components is enhanced leading finally to re-crystallization of the particular components to the ternary pseudobrookite phase, while the remaining fraction of the $Fe_2O_3$ conserves in the hematite phase.

TABLE I
RELATIVE CONTENT OF THE TITANIA AND IRON OXIDE PHASES, DETERMINED BY THE DEBYE METHOD

| *sample* | ana. | rut. | γ | α |
|---|---|---|---|---|
| S200 | 54±5 | 46±5 | 100 | x |
| S450 | 50±5 | 50±5 | 84±5 | 16±5 |
| S550 | 66±10 | 34±10 | 66±5 | 34±5 |
| S700 | 40±5 | 60±5 | 9±5 | 91±5 |
| S770 | x | 100 | x | 100* |

TABLE II
APPARENT PARTICLE DIAMATER OF THE PARTICULAR PHASES

| *sample* | ana *d*(nm) | rut *d*(nm) | γ *d*(nm) | α *d*(nm) |
|---|---|---|---|---|
| S200 | 5.3±1.2 | 7.0±0.7 | 10.1±1.2 | x |
| S450 | 5.0±0.8 | 6.2±0.8 | 10.8±1.7 | x |
| S550 | 6.5±1.2 | 6.2±1.3 | 12.0±1.2 | 6.6±0.9 |
| S700 | 9.5±2.4 | 5.0±1.9 | x | 12.6±1.1 |
| S770 | x | 5.0±0.9 | x | 23.9±2.1 |

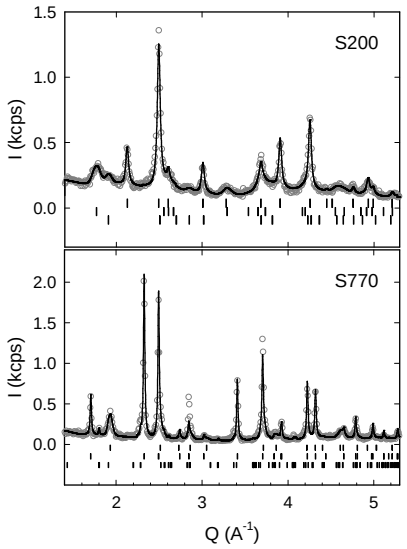


Fig. 1 Powder X-ray diffraction patterns of the S450 and S700 samples. The line corresponds to the fit by using the Rietveld refinement, the vertical lines mark positions of the phases included in the fit

### *B. Mössbauer spectroscopy*

Typical Mössbauer spectra of the S200 and S700 samples are presented in Figure 2. The spectrum of the S200 shows a saw-like character, which is a characteristic sign of maghemite in form of small particles and/or with a partial structural disorder. The spectrum was described by using two sextets, which do not represent two inequivalent Fe positions in the structure, but the approach is generally used for description of such maghemite systems. The two doublets can be attributed to the mahemite particles in the superparamagnetic state or close to the blocking temperature, as discussed further in the

Subection C. The spectrum of the S700 sample consists of a sextet with the parameters corresponding to the hematite, and a doublet attributed to the pseudobrookite. The spectrum of the sample S900 was analyzed in the same way. The obtained Mössbauer parameters are finally summarized in Table III. The relative ratio of the Fe-containing phases is slightly different form that obtained by the analysis of the S-PXRD data. This discrepancy can be explained by the fact, that the Debye method did not included the ternary phase in the analysis, and also the amount of the $Fe_2O_3$ or $Fe_2TiO_5$ determined from the area of the particular sub-spectra has an error of about 10 %.

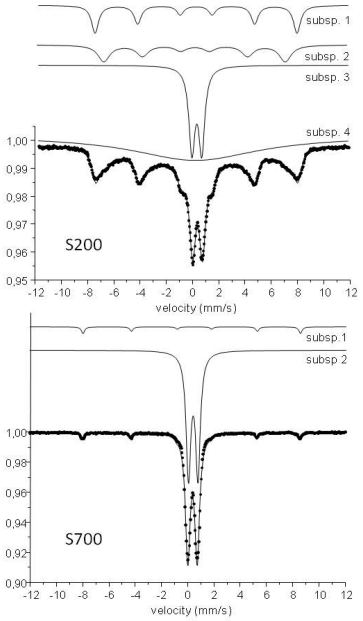


Fig. 2 Room temperature Mössbauer spectra of the S200 and S700 samples

TABLE III
RESULTS OF THE ANALYSIS OF THE RT MÖSSBAUER SPECTRA
*$\delta$ – ISOMER SHIFT, $\Delta E_Q$ - QUADRUPOLAR SPLITTING, $B_{HF}$ - HYPERFINE FIELD, % - RELATIVE AREA, $\gamma$ – MAGHEMITE, $\alpha$ – HEMATITE, PB - PSEUDOBROOIKITE*

| *sample subsp.* | $\delta$ (mm/s) | $\Delta E_Q$ (mm/s) | $B_{HF}$ (T) | % |
|---|---|---|---|---|
| S200 | | | | |
| 1 γ | 0.32 | -0.01 | 47.8 | 14 |
| 2 γ | 0.33 | -0.04 | 43.0 | 14 |
| 3 γ | 0.38 | 0.75 | N/A | 18 |
| 4 γ | 0.24 | N/A | N/A | 54 |
| S700 | | | | |
| 1 α | 0.37 | -0.21 | 51.4 | 6 |
| 2 pb | 0.37 | 0.72 | N/A | 94 |
| S900 | | | | |
| 1 α | 0.37 | -0.21 | 51.6 | 5 |
| 2 pb | 0.38 | 0.72 | N/A | 95 |

### *C. Magnetic characterization*

The zero field-cooled (ZFC) and field-cooled (FC) temperature dependencies of magnetization are demonstrated in Figure 3.

The ZFC-FC curves of the S200 and S550 samples show typical features of a superparamagnetic (SPM) system, demonstrated by the branching of the ZFC and FC curves at the effective blocking temperature about 350 K. The saturation of the FC curve on cooling suggests considerable dipolar interaction among particular nanocrystallites. The ZFC-FC curves of the S700 sample can be decomposed into two contributions, first one due to a remnant fraction of the maghemite particles with similar features as in case of the S200 and S550 samples, and second attributed to a paramagnetic like fraction. Considering the S-PXRD results, a significant contribution of the hematite, demonstrated by the Morin transition at $T_M$ = 263 K is expected. However, the particle size in the sample is about 12 nm and 24 nm, therefore the Morin transition vanishes in consistency with previous observations in hematite particles with size below 25 nm [10].

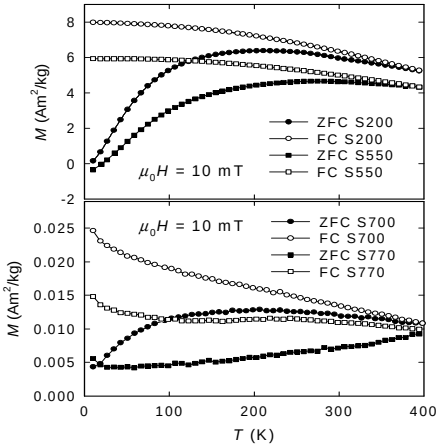


Fig. 3 Temperature dependencies of magnetization recorded in the zero field-cooled (ZFC) and field-cooled (FC) regime ($\mu_0 H$ = 10 mT)

The trend in magnetization is almost identical in case of the S770 sample, just the SPM-like contribution of maghemite lacks in agreement with the phase analysis.The ZFC-FC curves for the S900 sample are shown on Figure 4. The ZFC and FC curves branch at around 220 K. The observed effect is attributed to the Morin transition of the hematite fraction. The kink on the ZFC curve at around 80 K, and almost paramagnetic like character of the FC curve are typical features of the pseudobrookite, which is known as an anisotropic spin glass system [11].

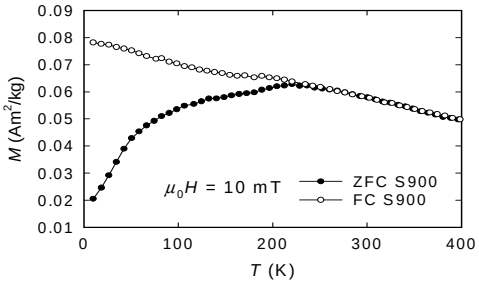


Fig. 4 Temperature dependence of magnetization recorded in the zero field-cooled (ZFC) and field-cooled (FC) regime ($\mu_0 H$ = 10 mT) of the S900 sample containing pseudobrookite and hematite

The SPM character of the particles in the samples annealed at lower temperatures was evidenced by additional experiments of the a.c. susceptibility, shown in Figure 5 for the S200. The shape of the real part, $\chi$' signalizes a size distribution of the nanoparticles in the sample and a moderate shift of the rather broad maximum of the $\chi$' and $\chi$'' curves points to a significant inter-particle interactions among the maghemite crystallites. Also the temperature of the $\chi$' - maximum is about 230 K, which is much lower value than the effective blocking temperature, $T_B^{eff}$ = 350 K, determined from the ZFC-FC curves, which is an additional sign of significant dipolar integrations between nanoparticles.

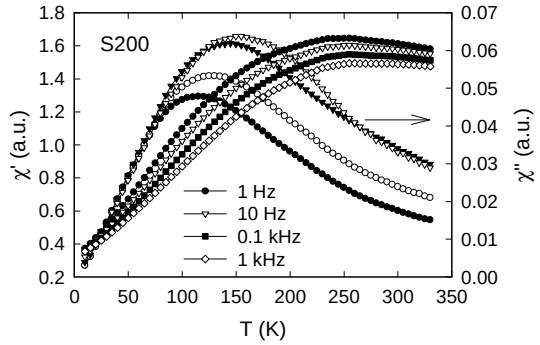


Fig. 5 real part of the a.c. susceptibility of the S200 sample

## IV. CONCLUSIONS

We have investigated phase composition and its relation to particle size and magnetic properties in the system of $Fe_2O_3$-$TiO_2$ obtained by heterogeneous precipitation of the $TiO_2$ on the surface of citric acid stabilized $Fe_2O_3$ nanocrystals. The sample dried at 200 $^oC$ consists of maghemite and anatase and rutile in approx. 1:1 ratio. When annealing the samples up to 700 $^oC$, the hematite phase forms and its content and particle size gradually increases with the increasing annealing temperature up to 24 nm and 95 % at 700 $^oC$, respectively. The content of the rutile also moderately increases, up to 60 % of the $TiO_2$ fraction at at 700 $^oC$, however the particle size of the $TiO_2$ phases is generally less affected. Investigations of magnetic properties are in consistency with the phase composition, determined by the X-ray diffraction and Mossbauer spectroscopy. The samples containing majority of the maghemite phase (S200, S450, S550) can be described as strongly-interacting superparamagnets, the samples with hematite (S700, S770) revealed lack of the Morin transition due to the small particle size, and the fully crystalline samples (S820, S900) show typical features of the pseudobrookite and ordered hematite. The obtained results suggest, that the samples treated at lower temperature (S450 and S550) are the best candidates for the photocatalysis combined with magnetic separation, as their magnetic activity is ensured by the interacting superparamagnetism, and content and particle size of the photocatalytic $TiO_2$ phases is sufficient.

## ACKNOWLEDGMENT

The work was supported by the Grant Agency of the Czech Republic, project no. P108/10/1250. The work is a part of the research plan MSM0021620857 that is financed by the Ministry of Education of the Czech Republic. We acknowledge the Synchrotron Light Source ANKA for provision of beamtime at the PDIFF.

## REFERENCES

[1] B. Pal, M. Sharon, G. Nogami, "Removal of natural organic matter from water using a nano-structured photocatalyst coupled with filtration membrane", *Mater. Chem. Phys*., vol. 59, pp. 254-261, 1999.

[2] J.A. Navio, G. Colon, M.I. Litter, G.N. Bianco, "Synthesis, characterization and photocatalytic properties of iron-doped titania semiconductors prepared from $TiO_2$ and iron(III) acetylacetonate", *J. Mol. Catal. A. Chem*., vol. 106, pp. 267, 1996.

[3] D. Sun, T.T. Meng, T.H. Loong, T.J. Hwa, "Removal of natural organic matter from water using a nano-structured photocatalyst coupled with filtration membrane", *Water Sci. Technol.*, vol. 19, pp. 315601, 2008.

[4] S.K. Mohapatra, S. Banerjee, M. Misra,, "Synthesis of $Fe_2O_3/TiO_2$ nanorod–nanotube arrays by filling $TiO_2$ nanotubes with Fe", *Nanotechnology*, vol. 49, pp. 103-110, 2004.

[5] J. Morales, L. Sanchez, F. Martin, F. Berry, X. Ren, "Synthesis and Characterization of Nanometric Iron and Iron-Titanium Oxides by Mechanical Milling: Electrochemical Properties as Anodic Materials in Lithium Cells", *J. Electrochem. Soc*., vol. 152, pp. A1748-A1754, 2005.

[6] V. Tyrpekl, J. P. Vejpravova, A. Roca, N. Murafa, L. Szatmary and D. Niznansky, "Magnetically separable photocatalytic composite g-$Fe_2O_3$@$TiO_2$ synthesized by heterogeneous precipitation", *Appl. Surf. Sci.*, vol. 257, pp. 4844-4848, 2011.

[7] B. E. Warren, *X-ray Diffraction*, Dover Publications, New York, 1990.

[8] V. Vales, J. P. Vejpravova, V. Holy, V. Tyrpekl, P. Brazda and S. Doyle, "Study of the phase composition of $Fe_2O_3$ and $Fe_2O_3/TiO_2$ nanoparticles using X-ray diffraction and Debye formula", *Phys. Status Solidi C*, vol. 7, pp. 1399-1404, 2010.

[9] J. Rodriguez-Carvajal, *FullProf User's Guide Manual*, CEA-CRNS, France, 2000.

[10] S.N. Klausem, K. Lefmann, P.-A. Lingard, L. T. Kuhn, C.R.H. Bahl, C. Frandsen, S. Morup, B. Roessli, N. Cavadini, C. Niedermayer, "Magnetic anisotropy and quantized spin waves in hematite nanoparticles", *Phys. Rev. B*, vol. 70, pp. 214411, 2004.

[11] S.N. Klausem, K. Lefmann, P.-A. Lingard, L. T. Kuhn, C.R.H. Bahl, C. Frandsen, S. Morup, B. Roessli, N. Cavadini, C. Niedermayer, "Magnetic anisotropy and quantized spin waves in hematite nanoparticles", *Phys. Rev. B*, vol. 70, pp. 214411, 2004.